TECHNICAL MEMORANDUM

819

A positive definite tracer mass fixer for high resolution weather and atmospheric composition forecasts

Michail Diamantakis and Anna Agusti-Panareda

Research Department

December 2017

European Centre for Medium-Range Weather Forecasts
Europäisches Zentrum für mittelfristige Wettervorhersage
Centre européen pour les prévisions météorologiques à moyen terme

Series: ECMWF Technical Memoranda

A full list of ECMWF Publications can be found on our web site under:
http://www.ecmwf.int/en/research/publications

Contact: library@ecmwf.int

European Centre for Medium-Range Weather Forecasts
Shinfield Park, Reading, RG2 9AX, England

Abstract

Recent high-resolution experiments with atmospheric composition forecasts using the IFS Bermejo & Conde tracer mass fixing scheme, revealed cases where the positive definiteness of the transport scheme was violated with negative values being introduced in the tracer. This occurs in near surface atmospheric levels in areas where the tracer substance is injected in the atmosphere, for example CO_2 and CH_4 anthropogenic emissions. Such emissions introduce a sharp increase in the concentration of the tracer field and, as a result of this, the asymptotic assumptions that guarantee monotonicity of the mass fixing scheme break down. In this report, the implemented in IFS Bermejo & Conde scheme is revisited and modified to guarantee positive definiteness. Alternative formulations are described which may have advantages for tracer fields which are localised and discontinuous in nature unlike long-lived carbon tracers which are well mixed with air and have large background values. The modified scheme is tested on idealised case studies, weather forecast cases and atmospheric composition forecasts of CO_2 and CH_4. Results from these tests re-enforce previous conclusions, showing clear improvements for simulations of CO_2 and CH_4 tracers and neutral results in terms of forecast skill when the mass fixer is applied to specific humidity field. The impact on water vapour transport of two quasi-monotone interpolation limiters available in IFS is also analysed and their aparent "moistening effect" is explained.

1 Background

In Integrated Forecast System (IFS) atmospheric composition forecasts a mass fixer is used to keep the global mass of the long-lived CO_2 and CH_4 tracers constant during the semi-Lagrangian advection step. This is necessary given that these two tracers are not sufficiently constrained by observations and without a mass fixer, conservation error can accumulate in a period of few months deteriorating the forecast quality. Tracer mass fixer algorithms were introduced in IFS cycle 39r1. This development was refined in the following cycles optimizing and improving the flexibility of the mass fixer package. Testing showed a clear benefit in using the Bermejo & Conde (BC) mass fixer (MF) for high resolution CO_2 and CH_4 forecasts (see Agusti-Panareda et al., 2017). Not only the mass of the tracers remained constant during the advection step but the mean error was reduced by a factor of approximately 3 when measured against a set of station observations.

The IFS Bermejo & Conde MF scheme, Diamantakis and Flemming (2014); Agusti-Panareda et al. (2017), is an evolution of the original algorithm by Bermejo and Conde (2002). This scheme, for sufficiently smooth fields, remains positive definite and shape preserving which means it does not generate new minima/maxima. However, model runs at 9km resolution (TCo1279) showed that this is no longer the case i.e. the fixer can occasionally generate negative specific ratios. This happens in regions of strong point emissions which mathematically can be considered as discontinuities and invalidate the asymptotic assumptions that ensure positivity and shape preservation of the original algorithm. It was therefore necessary to reformulate the scheme ensuring that the solution remains always positive definite. A modified version has been introduced in cycle 45r1 which is described here.

2 The Bermejo & Conde mass fixer algorithm in IFS

The BC MF in IFS adjusts the mass of a tracer at each model grid-point, after semi-Lagrangian advection, to ensure that the global mass before and after advection does not change. It computes a correction to the transported field with magnitude depending on the local smoothness of the field; in regions of the atmosphere where the transported field is nearly constant or changes smoothly the correction is very

small while it is larger otherwise. The correction is the analytical solution of a constrained minimization problem; for details see section 3.1 in Diamantakis and Flemming (2014). The method described in the previous paper was modified in cycle 43r1 incorporating a vertical scaling of the mass fixer weight to take into account the strong vertical variation of the tracer mass. Furthermore, a more flexible specification of the mass fixer weight was introduced which allows tuning according to the spatial characteristics of a particular tracer; for example if it is widespread and well-mixed or more localised in nature. These changes were clearly beneficial for CO_2 and CH_4 forecasts as shown by the results discussed in Agusti-Panareda et al. (2017).

The IFS BC MF algorithm for a tracer ϕ can be briefly described by the equations:

$$\phi_{jk} = \phi^{adv}_{jk} - \lambda w_{jk}, \quad \lambda = \frac{\delta M}{\sum_{j=1}^{N} A_j \sum_{k=1}^{K} w_{jk} \frac{\Delta p^{adv}_{jk}}{g}}, \tag{1}$$

where N, K are the number of grid-points per level and the number of vertical levels respectively, j, k the horizontal and vertical level index of a grid-point, (ϕ^{adv}, p^{adv}) is the tracer specific ratio and the pressure field after the SL advection step and δM denotes the global mass error:

$$\delta M = M(\phi^{adv}, p^{adv}) - M(\phi^0, p^0)$$

where (ϕ^0, p^0) are the tracer mass and pressure at the beginning of a time-step. In IFS, the global mass is calculated as follows:

$$M(\phi, p) = \sum_{j=1}^{N} A_j \sum_{k=1}^{K} \phi_{jk} \frac{\Delta p_{jk}}{g}. \tag{2}$$

The mass fixer weight w_{jk} is specified as:

$$w_{jk} = \max\left[0, sgn(\delta M) sgn\left(\phi^{adv}_{jk} - \phi^{L}_{jk}\right) \left|\phi^{adv}_{jk} - \phi^{L}_{jk}\right|^{\beta} s_{jk}\right], \quad s_{jk} = \frac{p_{jk}}{p_{j0}}. \tag{3}$$

This weight depends on the difference between the cubic interpolated field ϕ^* and the linear interpolated ϕ^L, both at the departure point, and determines the size of the mass fixer correction: in areas where the tracer field does not change the computed weight is close to 0 while it is larger otherwise. The parameter β is a tracer dependent parameter which influences further the magnitude of the weight (3): using $\beta > 1$ results in even larger corrections for grid-point values lying in areas with sharp gradients. Testing has shown (Agusti-Panareda et al., 2017) that for CO_2 and CH_4, $\beta = 2$ is an appropriate value while for other species which are not well mixed with air but more localised in nature $\beta \leq 1$ is a more appropriate choice. The scaling factor s_{jk} ensures that corrections are larger at lower levels where the tracer mass is larger. The presence of the sign function in the weight implies that in the case that semi-Lagrangian advection increases the global mass of the tracer i.e. $\delta M > 0$ then only grid-points with $\phi^{adv}_{jk} > \phi^{L}_{jk} \geq \phi_{min} \geq 0$ are corrected by reducing their mass (to eliminate global mass error). Those grid-points where $\phi^{adv}_{jk} < \phi^{L}_{jk}$ are not modified to reduce the risk of introducing new minimum values or even negatives. The opposite is true when $\delta M < 0$ i.e. mass can only be added when $\phi^{adv}_{jk} < \phi^{L}_{jk}$ and never removed.

Having sufficiently small mass fixer corrections ensures that no new local minima or local maxima are produced. However, for tracer fields which have regions with steep gradients, there is no guarantee that the fixer will preserve local monotonicity or even positivity especially if $\beta > 1$. This situation actually occurs in high resolution CO_2 and CH_4 composition forecasts near surface levels in regions of emissions where the steepest tracer gradients are observed. To overcome this problem the BC MF algorithm was revised as shown in "Algorithm 1" by embedding a limiter (see step 4). An additional correction is

Algorithm 1 Quasi-monotone BC MF algorithm

1. Compute mass error: $\delta M = M(\phi^{adv}, p^{adv}) - M(\phi^0, p^0)$
2. Compute weight:

   $w_{jk} = \max\left[0, sgn(\delta M) sgn\left(\phi^{adv}_{jk} - \phi^L_{jk}\right) \left|\phi^{adv}_{jk} - \phi^L_{jk}\right|^\beta s_{jk}\right],\ s_{jk} = A_j \Delta p_{jk},\ A_j$: horizontal area weight
3. Apply MF: $\phi^{mf}_{jk} = \phi^{adv}_{jk} - \lambda w_{jk}, \quad \lambda = \dfrac{\delta M}{\sum_{j=1}^{N} A_j \sum_{k=1}^{K} w_{jk} \frac{\Delta p^{adv}_{jk}}{g}}$
4. Apply limiter: $\phi^{mfl}_{jk} = \min(\phi_{max}, \max(\phi_{min}, \phi^{mf}_{jk}))$; ϕ_{min}, ϕ_{max}: local min, max for grid-point jk
5. Compute global mass of corrected field: $M(\phi^{mfl}, p^{adv})$
6. Correct any new (very small) mass conservation error the limiter may have introduced by applying proportional mass fixer:

$$\phi^{cons}_{jk} = M(\phi^{mf}, p^{adv}) / M(\phi^{mfl}, p^{adv}) \phi^{mfl}_{jk} = M(\phi^0, p^0) / M(\phi^{mfl}, p^{adv}) \phi^{mfl}_{jk}$$

Algorithm 2 Positive definite BC MF algorithm

1. Compute mass error: $\delta M = M(\phi^{adv}, p^{adv}) - M(\phi^0, p^0)$
2. Compute weight:

$$w_{jk} = \left|\phi^{adv}_{jk} - \phi^L_{jk}\right|^\beta s_{jk},\ s_{jk} = A_j \Delta p_{jk},\ A_j : \text{ horizontal area weight}$$
3. Apply MF: $\phi^{mf}_{jk} = \phi^{adv}_{jk} - \lambda w_{jk}, \quad \lambda = \dfrac{\delta M}{\sum_{j=1}^{N} A_j \sum_{k=1}^{K} w_{jk} \frac{\Delta p^{adv}_{jk}}{g}}$
4. Apply positive-definite limiter: $\phi^{mfl}_{jk} = \max(\varepsilon_\phi, \phi^{mf}_{jk})$, ε_ϕ: lowest permissible value for ϕ
5. Compute global mass of corrected field: $M(\phi^{mfl}, p^{adv})$
6. Correct any new (very small) mass conservation error the limiter may have introduced by applying proportional mass fixer:

$$\phi^{cons}_{jk} = M(\phi^{mf}, p^{adv}) / M(\phi^{mfl}, p^{adv}) \phi^{mfl}_{jk} = M(\phi^0, p^0) / M(\phi^{mfl}, p^{adv}) \phi^{mfl}_{jk}$$

entered (steps 5, 6) to ensure that a very small loss of global mass conservation which may occur from application of the limiter (which changes the already "conservatively adjusted" tracer field) is restored by applying a simple proportional MF algorithm. Similar attempts to ensure positivity of the BC or similar MF algorithms have been implemented by Grandpre et al. (2016).

If positive definiteness rather than the stricter shape preservation property is required then "Algorithm 2" can be used which is the IFS adaptation of the Zerroukat (2010) MF (see Diamantakis and Flemming, 2014). Typically, for both Algorithm 1 and 2, testing with different species shows that approximately 99% of the mass correction can be accounted to step 3 and 1% to step 6. So, the final adjustment is tiny and a positive definite shape preserving scheme remains positive definite and approximately shape preserving.

2.1 Alternative formulations for BC MF

The BC fixer algorithm described earlier in this section is additive in nature i.e. a mass conserving field is computed by adding a small correction in the transported field. It can be changed to restore conservation by multiplying the transported field with a small, grid-point value dependent, correction factor. The multiplicative approach works better for localised fields; this will be demonstrated in the section that follows. The proposed reformulation only requires a modification in the weight defined by equation (3) i.e. to multiply it by the specific ratio of the field

$$\widehat{w}_{jk} = \max\left[0, sgn(\delta M) sgn\left(\phi^{adv}_{jk} - \phi^{L}_{jk}\right) \left|\phi^{adv}_{jk} - \phi^{L}_{jk}\right|^{\beta} \phi^{adv}_{jk}\, s_{jk}\right] = w_{jk}\phi^{adv}_{jk} \tag{4}$$

which implies

$$\phi^{mf}_{jk} = \phi^{adv}_{jk} - \lambda\widehat{w}_{jk} = \phi^{adv}_{jk} - \lambda w_{jk}\phi^{adv}_{jk} = (1-\lambda w_{jk})\phi^{adv}_{jk}$$

The quantity $1-\lambda w_{jk}$ is a multiplication factor close to 1. If monotonicity is not required, then a simpler expression for the weight can be used which results in a positive scheme such as the one described by Algorithm 2:

$$\widehat{w}_{jk} = \left|\phi^{adv}_{jk} - \phi^{L}_{jk}\right|^{\beta} \phi^{adv}_{jk}. \tag{5}$$

The "multiplicative form" of Algorithms 1, 2 is obtained by replacing the weights w_{jk} in step 2 by expressions (4), (5) respectively. For $\beta \to 0$, equation (5) implies that $\widehat{w}_{jk} \to \phi^{adv}_{jk}$. Therefore, taking into account the definition of λ from step 3 or (1) we obtain:

$$\phi^{mf}_{jk} = \phi^{adv}_{jk} - \lambda\widehat{w}_{jk} = \left[1 - \frac{M(\phi^{adv}, p^{adv}) - M(\phi^{0}, p^{0})}{M(\phi^{adv}, p^{adv})}\right]\phi^{adv}_{jk} = \frac{M(\phi^{0}, p^{0})}{M(\phi^{adv}, p^{adv})}\phi^{adv}_{jk}$$

i.e the mass fixer converges to a simple un-weighted proportional mass fixer.

3 An idealised high resolution test

To assess the performance of mass fixers in very small scales we use the small planet high resolution dry bubble tracer test case by Malardel and Ricard (2015). In this case, the radius of the Earth is reduced by a factor of 100 corresponding to horizontal resolution of 1.25km approximately while 137 levels are used in the vertical. In an atmosphere initially at rest, there is a bubble shape warm anomaly at the lowest 4 levels with a tracer embedded in the warm bubble. Following Malardel and Ricard (2015), the bubble is simulated for 2 hours with a time-step of 10s. This case exposes how severe the problem of mass

conservation in a semi-Lagrangian advection scheme can be come under very special conditions and at high resolution: after 720 time-steps the initial mass of the tracer increases by a factor close to 20.

A vertical cross section of the tracer mass specific ratio is plotted in Fig. 1 for different simulations: (a) with the standard IFS semi-Lagrangian scheme (b) as before but with BC MF Algorithm 1 (additive MF) with $\beta = 1$ (c) with the multiplicative version of BC MF described in section 2.1 with $\beta = 1$ and (d) with the multiplicative BC MF and $\beta = 0.2$. The mass fixer keeps the total mass constant and this is reflected by the lower values of specific ratios in the plots. However, the response of the different versions varies. The default BC removes a lot of mass near the top: given the very small area of the advected bubble the fixer acts strongly in the region of sharpest gradient (top part of bubble) removing too much mass from there. This improves when switching to the multiplicative version as it is illustrated in Fig. 1c, d. This test is also a severe test for the positivity of the algorithm. It is noted that BC MF versions up to cycle 43r3 produced a lot of negative values while the modified versions described here remained always positive which confirms the success of the modifications described in this report.

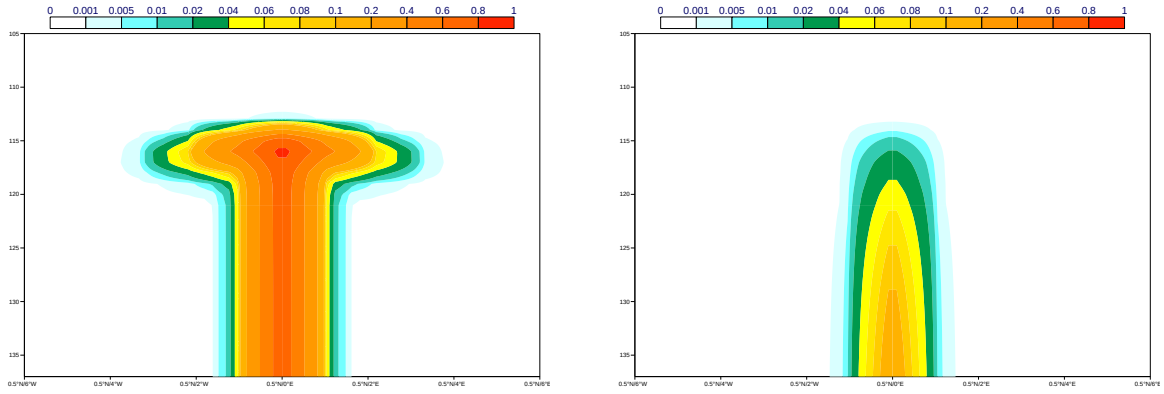

(a) No fixer

(b) BC fixer

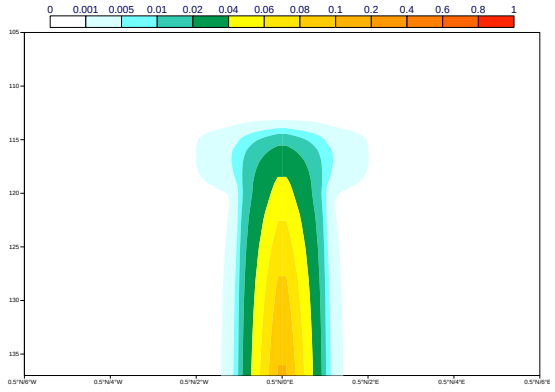

(c) Multiplicative BC fixer $\beta = 1$

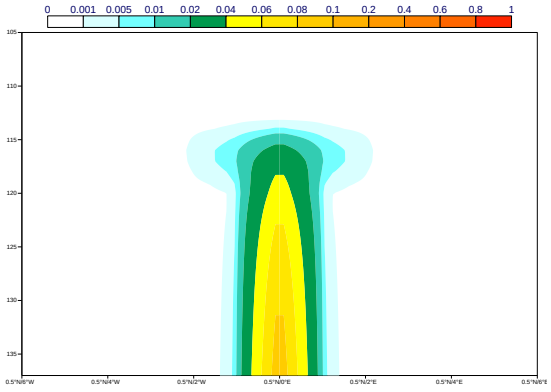

(d) Multiplicative BC fixer $\beta = 0.2$

Figure 1: Bubble tracer test case. East-west vertical cross-section for tracer specific ratio at t+2hrs for simulations without MF and different versions of MF BC.

4 Forecast case studies

The BC MF has also been tested on the specific humidity field (q) running high resolution (9km) forecast cases. Specific humidity mass fixer increments at t+24 hrs step, from a model level at approximately 850 hPa geopotential height over the sea and from a forecast case starting at 00UTC 1 January 2017 are shown in Fig. 2. These are computed from the default IFS (additive) BC fixer and revised (multiplicative) BC fixer. Both versions of this algorithm compute localised corrections which have a very small magnitude (4-5 orders of magnitude smaller than the magnitude of the actual q-field). The correction computed by the multiplicative version is even smaller (negligible) in the driest areas of the globe.

Activating the BC MF on specific humidity in a TCo1279 (9km) winter forecast experiment (40 cases), produced broadly neutral or slightly positive verification results in terms of 500 hPa geopotential root mean square error (rmse) as shown in Fig. 3. Similar results are obtained from an equal number of summer cases (not shown here). In the experiment represented by the black curve, the default BC MF (additive version) is combined with the standard Bermejo and Staniforth (1992) 3D quasi-monotone limiter. In the experiment represented by the red curve, BC MF is combined with the default IFS specific humidity quasi-monotone limiter. The latter is based in the same idea as the 3D limiter, however, it limits separately the result of each 1D cubic interpolation which takes place in the 3D computational stencil (east-west, north-south, bottom-up, see Ritchie et al., 1995) rather than limiting the final result of 3D interpolation. Both experimental runs are compared against a control run which does not use any fixer while it is using the default limiter.

These forecast cases also show that while the 500 hPa anomaly correlation coefficient and the standard deviation of geopotential error remain constant, the rmse in the tropical troposphere increases as the corresponding temperature error increases (not shown here). The latter is associated with an existing negative temperature bias in the region and a further small drop in the mean temperature linked to a reduction of water vapour content from the tracer mass fixer (see also section 4.2 in Diamantakis and Flemming, 2014). Semi-Lagrangian advection increases slightly the total mass of water vapour and the fixer removes the excess to conserve global mass (see Fig. 2). Furthermore, replacing the default IFS limiter by the 3D limiter has an additional to the mass fixer drying effect in the atmosphere which is even stronger if no limiter is used. This is also confirmed in runs without MF. In other words, limiters result in moistening. Fig. 4 shows the effect of the MF and the 3D limiter in the atmospheric water content.

To explain the aparent "moistening effect" of the advection limiters, we note that an amount of water vapour is "implicitly added" in the atmosphere when the cubic interpolation undershoots are "clipped", to ensure that the interpolated value at the departure point is no less than its local minimum value. It turns out that the total water vapour mass clipped due to undershoots exceeds the corresponding total mass clipped due to overshoots, thus the limiter has a net "moistening effect". This feature is stronger in the default IFS limiter which is more active than the 3D limiter as the former operates in each of the 7 cubic interpolations of the 3D quasi-cubic, 32-point stencil interpolation algorithm (see Ritchie et al., 1995). Hence, with respect to the default IFS limiter the 3D limiter has a drying effect. Figure 5 illustrates this point for a summer and a winter forecast. The time-averaged vertically integrated water vapour mass correction, computed from the specific humidity limiter in the first 24 hours of a summer and a winter forecast, is plotted as a percent of the average total column water vapour in the 24 hrs period. The difference between the two versions of the limiter is noticeable with the default limiter being more active particularly in the main orographic belts. The 3D limiter adds approximately one half of the amount of water vapour added by the default limiter. Furthermore, the time-series plot of the mass fixer correction in Fig. 6 shows that when the 3D limiter is used the mass conservation error reduces by approximately 30%.

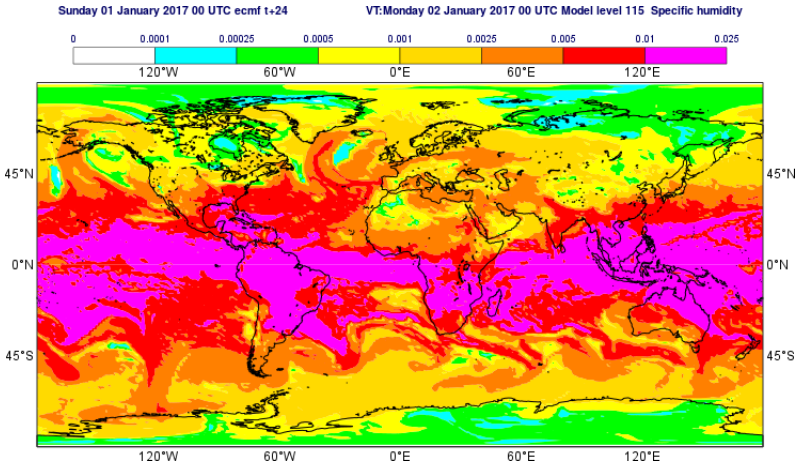

(a) Q at model level 115

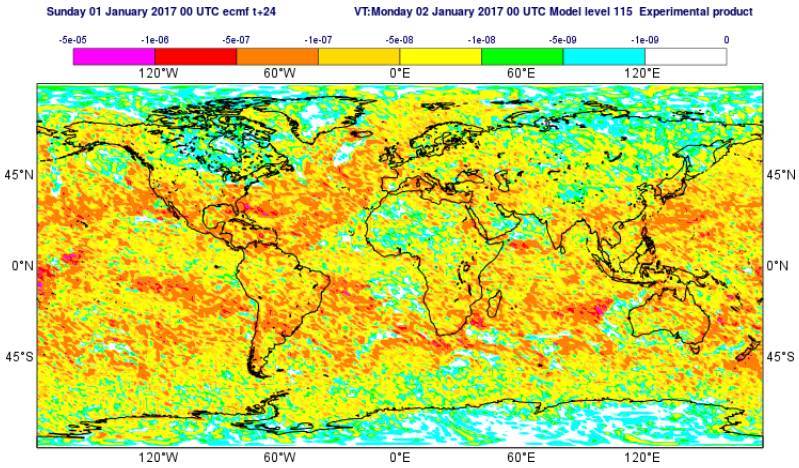

(b) BC MF correction for specific humidity at model level 115

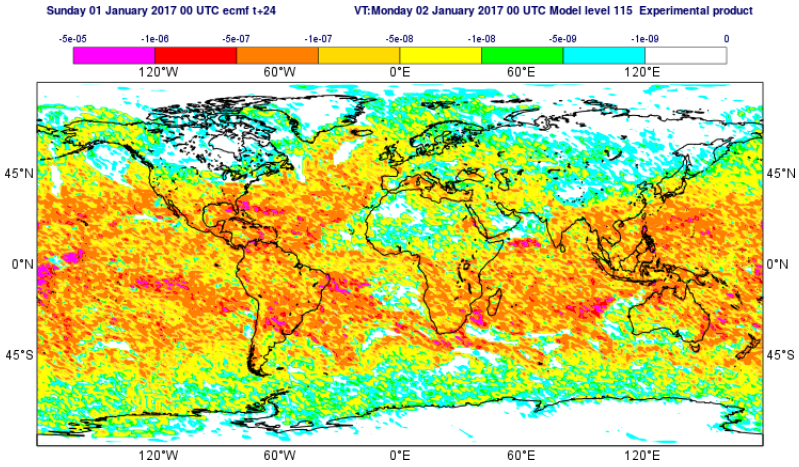

(c) BC MF (multiplicative) increment for q at model level 115

Figure 2: BC "additive" and BC "multiplicative" fixer mass correction for q at t+24 hrs and near 850 hPa height from a TCo1279 forecast with 137 vertical levels. Both with $\beta = 1$. All units in kg/kg (kg of water vapour per kg of air).

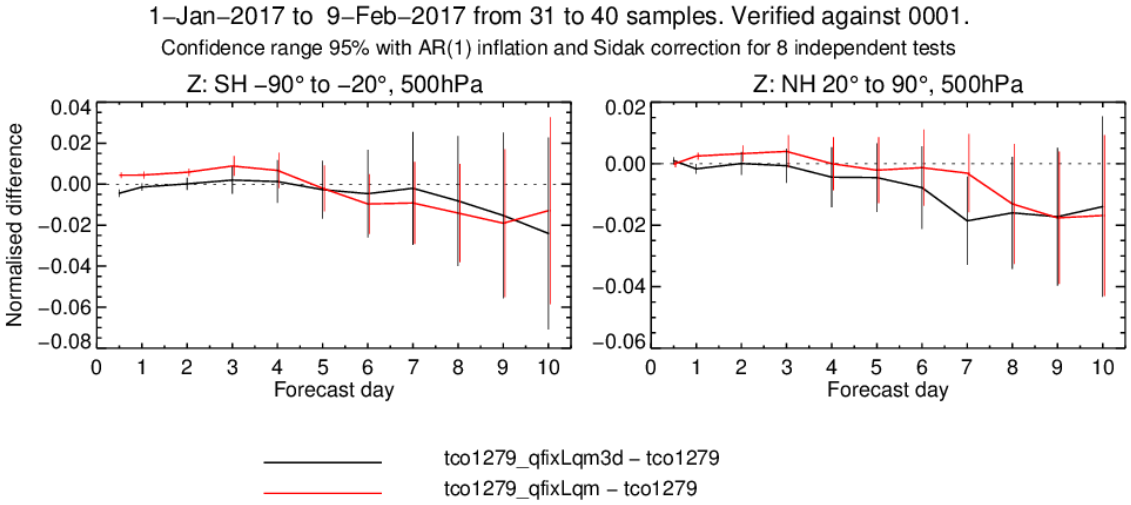

Figure 3: Difference in RMSE for the geopotential field at 500 hPa for an experiment (40 winter cases) using BC MF on specific humidity with default IFS limiter (red line) and 3D limiter (black line) against a control run without MF and with the standard IFS limiter. Negative values indicate improvement against the control and positive deterioration. The bar indicates the confidence interval.

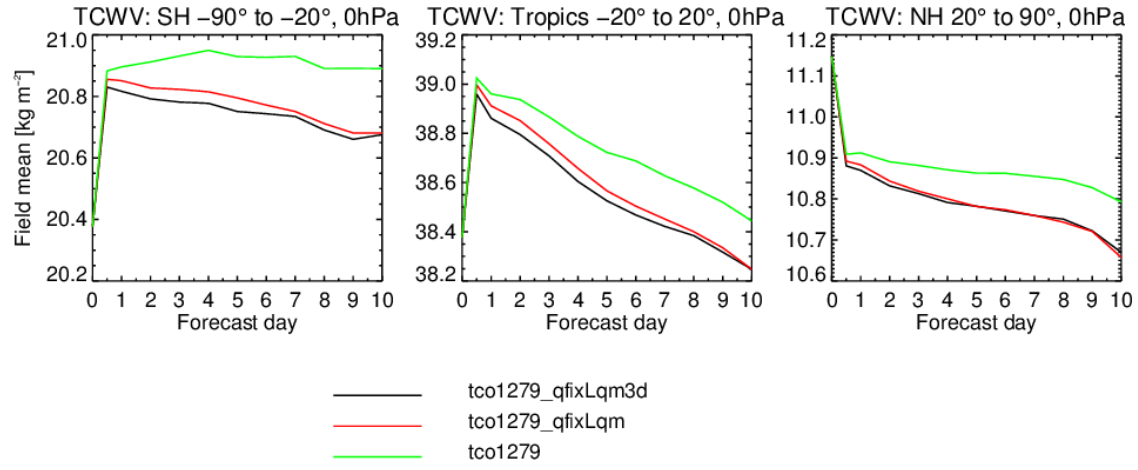

Figure 4: Total column water vapour time-mean for the northern hemisphere, the tropics and the southern hemisphere, for three 10-day forecast experiments (31 consecutive winter forecasts): (i) forecast with default limiter and without MF (green line) (ii) forecast with BC MF and default limiter (red line) and (iii) BC MF with 3D limiter (black line). There is a small additional "drying effect" when using the 3D limiter.

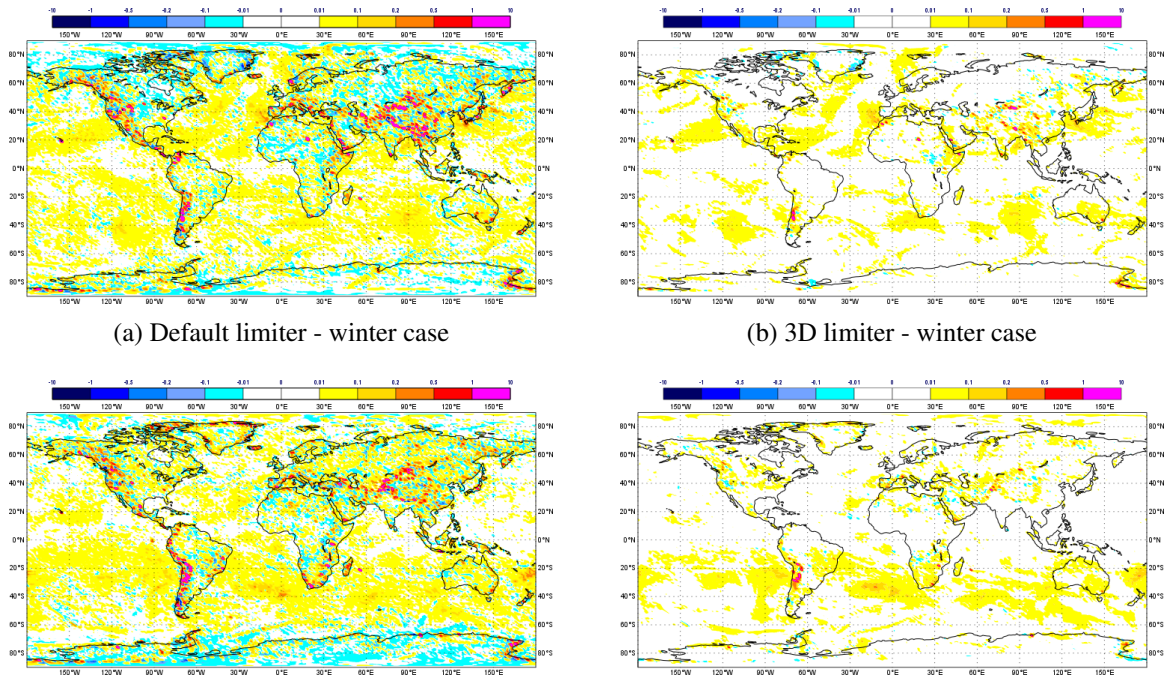

(a) Default limiter - winter case

(b) 3D limiter - winter case

(c) Default limiter - summer case

(d) 3D limiter - summer case

Figure 5: Vertically integrated water vapour mass correction per hour (kg/m^2/hr) as a percent of the total water vapour content from the cubic interpolation limiter of IFS sampled from the first 24 hours of two forecasts starting from 15/01/2017 and 15/07/2017 at 00 UTC.

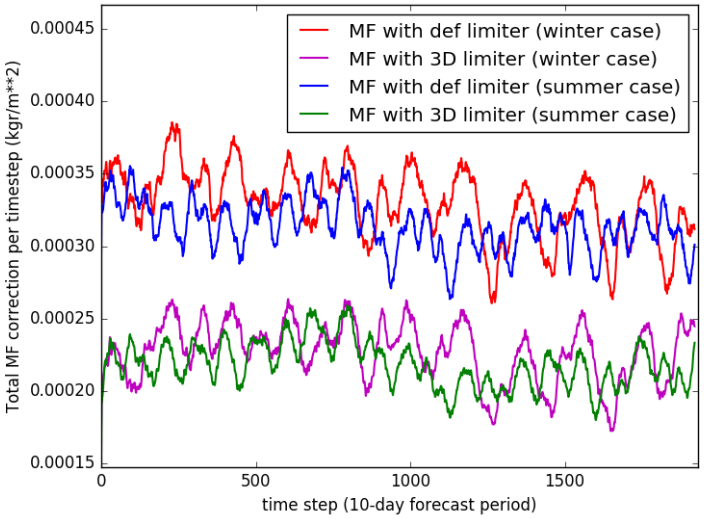

Figure 6: Time series of total global MF correction (kgr/m^2) for the default IFS limiter and for the 3D limiter applied to specific humidity field for two 10-day forecasts from 15/01/2017 00UTC and 15/07/2017 00UTC.

5 CO_2 and CH_4 atmospheric composition forecasts

Validation of CO_2 and CH_4 atmospheric composition forecasts with the updated BC scheme against observations shows that the mass fixer improves the quality of these forecasts. The experiments described in Agusti-Panareda et al. (2017) have been repeated using the high resolution TCo1279 (9km) model with the 3D monotone limiter and with the standard (additive) version of BC MF. This is appropriate given the nature of these tracers, i.e. well mixed with large background values and generally smooth gradients. At high resolution, the IFS BC MF scheme described in Agusti-Panareda et al. (2017) was occasionally producing negative concentrations for these tracers in regions of strong emissions. This problem was solved with the updated scheme described here. Furthermore, the mass fixer improved the quality of the simulation, restoring the global mass conservation and reducing the mean error of the semi-Lagrangian transport scheme for CO_2 and CH_4, particularly in the southern hemisphere (see Fig 7). It is also interesting to point out that the octahedral grid simulation TCo1279 without any MF is more accurate than the corresponding linear grid TL1279 both in terms of mass conservation error and mean error as illustrated by Figs. 8, 7. It is known, Malardel et al. (2014), that the octahedral grid has higher effective resolution, superior filtering properties and improved mass conservation properties compared to the linear grid. The improved accuracy of the wind fields result in improved departure point accuracy and therefore improved accuracy of the corresponding continuity equation that the tracer obeys. This is more noticeable for smoother well-mixed tracers rather than for tracers with sharp discontinuities. For the latter, large interpolation errors give rise to large mass conservation errors.

The mass fixer correction can also be monitored in the Copernicus Atmosphere Monitoring Service (CAMS) forecast of CO_2 and CH_4 with TCo1279 resolution and 137 vertical levels. This is done by computing the difference between CO_2 and CH_4 tracers with mass fixer and the equivalent tracers without the mass fixer throughout the 5-day forecast. All tracers are re-initialized with the CAMS analysis at the beginning of each forecast. An example of the mass fixer correction applied to a 1-day and 5-day October 2017 CAM operational forecast is shown in Fig. 9 for the column-mean dry molar fraction of the two tracers (XCO_2 and XCH_4). The current corrections are indeed very small in the background air away from strong sources/sinks: less than 0.01% for XCO_2 and less than 0.1% for XCH_4. However, in the vicinity of the strongest surface fluxes the mass fixer correction can reach up to 1% and 10% for XCO_2 and XCH_4 respectively in the 5-day forecast. Although it may appear small, this can be of similar magnitude to the atmospheric signal of anthropogenic emissions ranging from 0.01% to 1 % for XCO_2 and from 0.1% to 10% for XCH_4 as shown in the 1-day and 5-day forecasts (see left panels in Fig 10). The panels on the right in Fig 10 depict the difference in magnitude between the anthropogenic signal and the mass fixer correction for the 1-day and 5-day forecasts. Positive values indicate the anthropogenic signal is larger than the mass fixer correction. The fact that the positive patterns and magnitudes are similar to those from anthropogenic signal is reassuring. It implies the mass fixer correction is not introducing artifacts that might mask the anthropogenic signal. Whereas negative values shown in blue highlight regions where the mass fixer magnitude is larger than the anthropogenic signal, e.g. over the oceans, west coast of America, south America and Africa. These latter regions have to be monitored more closely because over those regions the relative uncertainty of the transport with respect to the anthropogenic signal is large.

The reference to the anthropogenic signal is important because this is the signal that top-down monitoring systems of anthropogenic greenhouse gas emissions aim to detect. It is therefore crucial to keep evaluating and assessing the performance of the mass fixer as part of ongoing efforts to reduce transport uncertainties associated with the anthropogenic emission signals in the atmosphere.

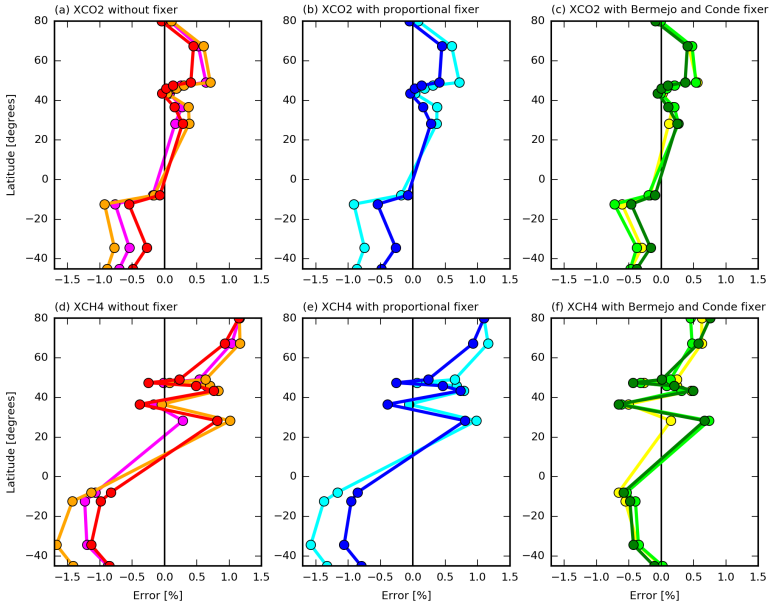

Error against TCCON

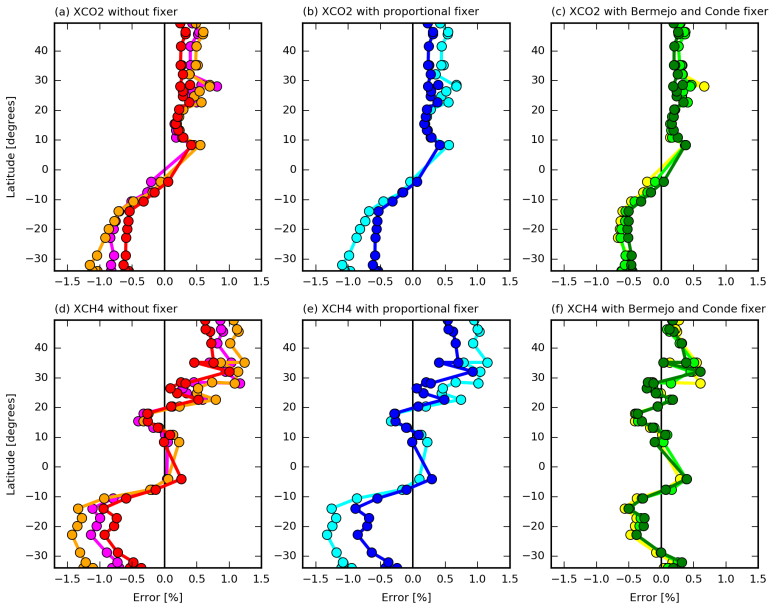

Error against Polastern

Figure 7: Error (%) of modelled latitudinal monthly mean distribution at the end of the forecast period (7 March to 10 April 2014) computed as $((MODEL - OBS) - \overline{(MODEL - OBS)})/OBS$ using different tracer mass fixers and different resolutions for (a-c) XCO_2 and (d-f) XCH_4 with respect to the observed distribution from TCCON (Wunch et al., 2011) and Polarstern (Klappenbach et al., 2015). Orange: TL255 (80km) simulation without MF, Red: TL1279 (16km) without MF, Magenta: TCo1279 (9km) without MF at low and high resolution respectively. Cyan and Blue: TL1279 (16km) and TL255 (80km) with proportional MF respectively. Green, light green and yellow: TL255 (80km), TL1279 (16km) and TCo1279 (9km) simulations with revised BC MF. XCO_2 and XCH_4 are the atmospheric column-averaged dry molar fractions of CO_2 and CH_4.

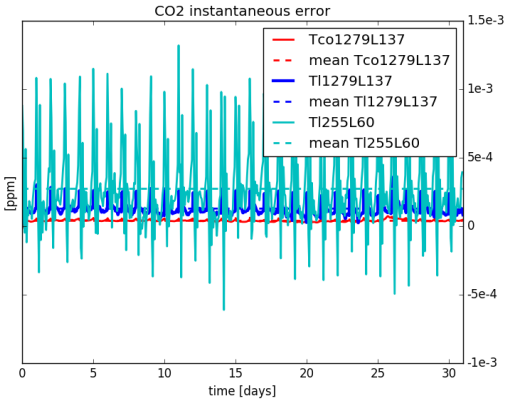

CO_2 instantaneous mass conservation error

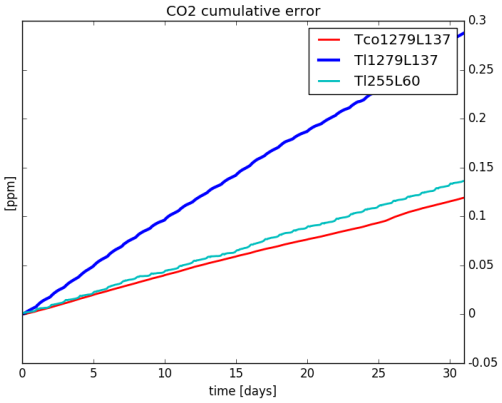

CO_2 cumulative mass conservation error

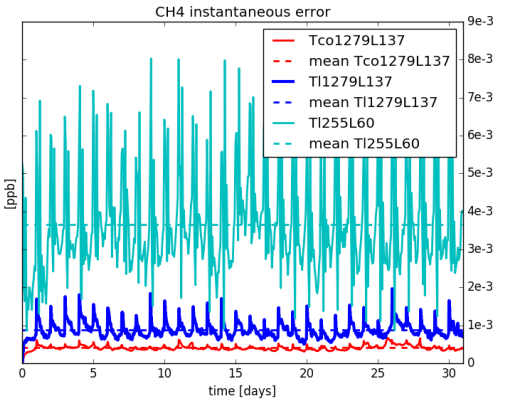

CH_4 instantaneous mass conservation error

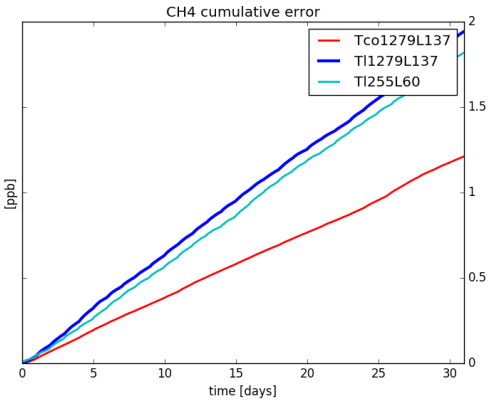

CH_4 cumulative mass conservation error

Figure 8: Instantaneous and cumulative mass conservation error for CO_2 and CH_4 24 hrs forecasts for a 30-day period during March 2013 at three different resolutions: TL255 (80km), TL1279 (16km), TCo1279 (9km). All experiments without mass fixer.

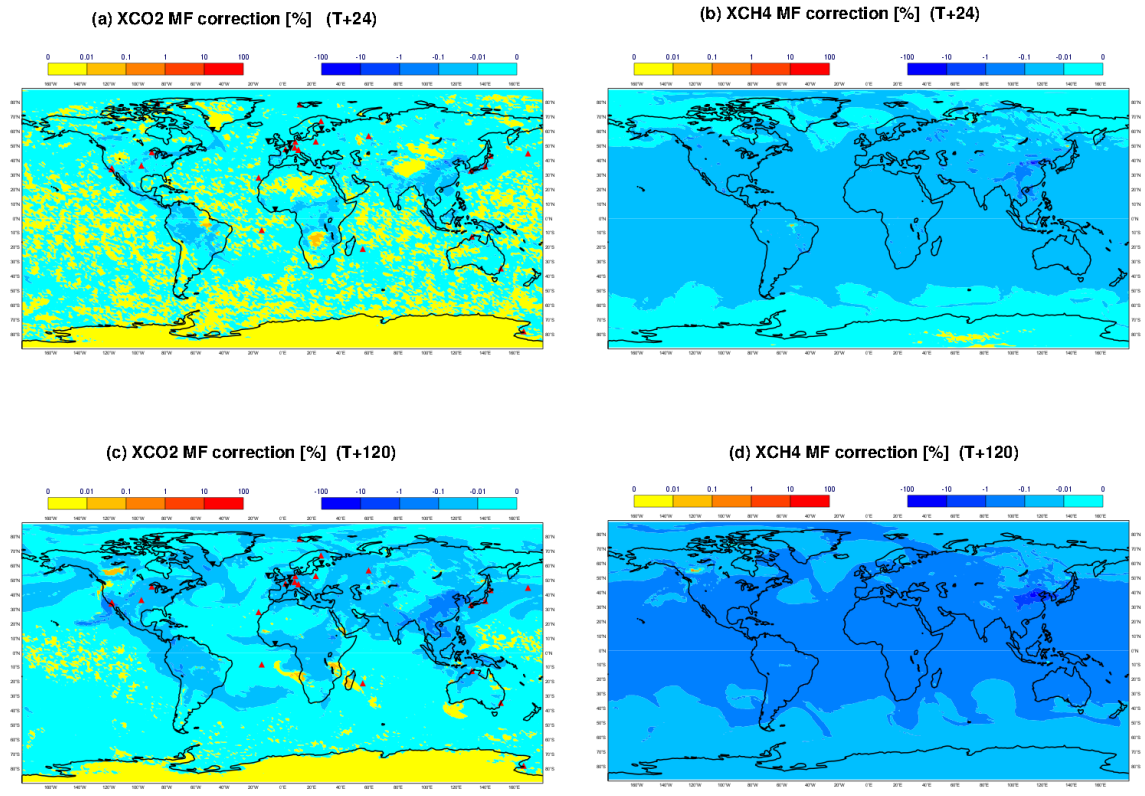

Figure 9: Mass fixer correction as percentage of XCO_2 and XCH_4 column-averaged dry molar fraction for 1-day (T+24) and 5-day (T+120) forecast of valid at 00 UTC 15 October 2017.

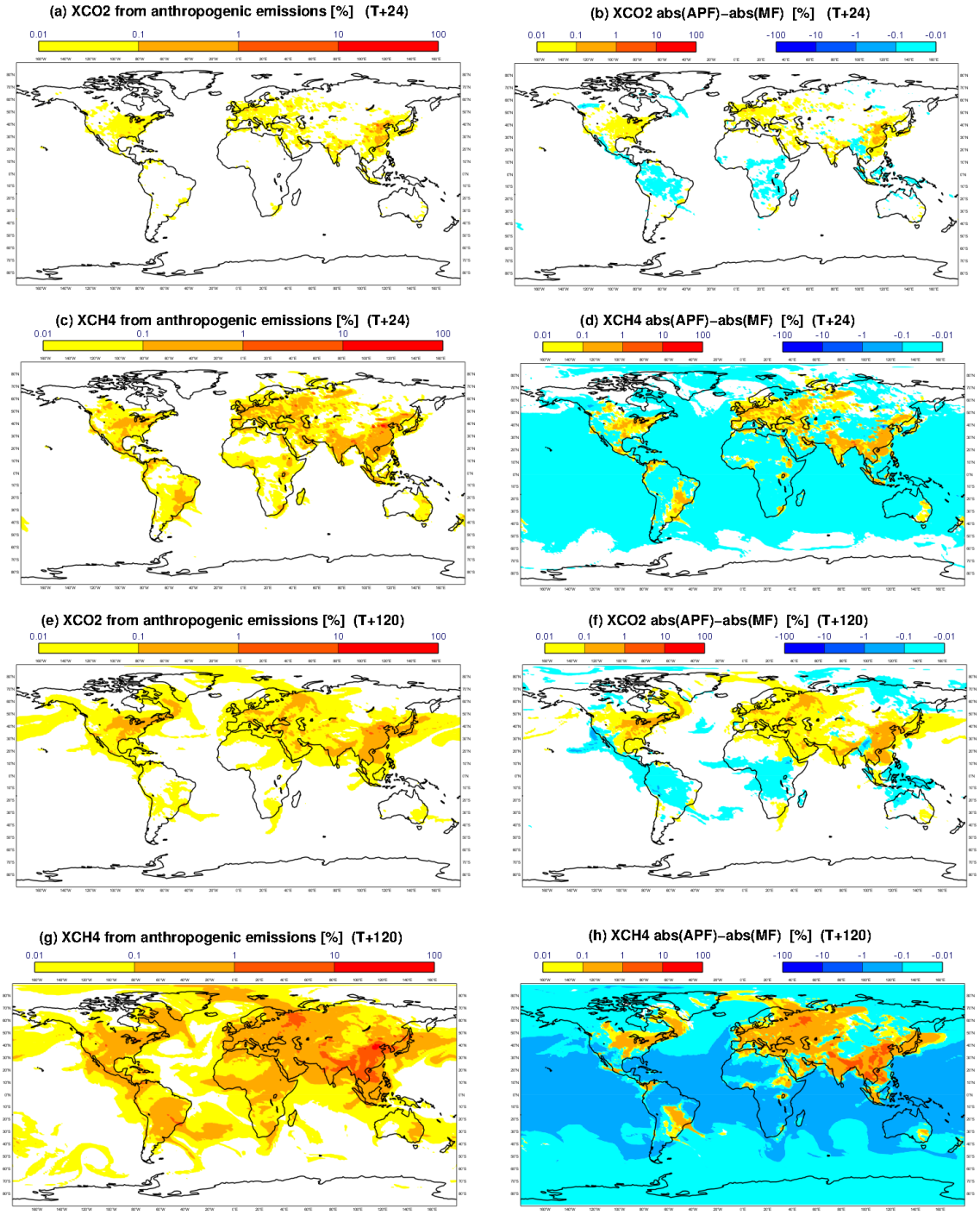

Figure 10: Left panels: enhanced XCO_2 and XCH_4 associated with anthropogenic fossil fuel emissions as a fraction of XCO_2 [%] during a 1-day (T+24) (a,b) and 5-day (T+120) (c,d) forecast valid at 00 UTC 15 October 2017; right panels: difference in magnitude between the XCO_2 and XCH_4 anthropogenic (APF) enhancement (shown in left panels) and mass fixer (MF) correction (shown in Fig 9) (in %) for the 1-day (a,b) and 5-day (c,d) forecast valid at 00 UTC 15 October 2017.

6 Concluding remarks

High resolution tests with the IFS Bermejo & Conde mass fixer algorithm have revealed cases where spurious negative concentrations were introduced in the simulated tracer. The IFS scheme has been modified in cycle 45r1 to guarantee positive definiteness and shape preservation (if the monotone limiter is used). Furthermore, an alternative form of this scheme has been introduced which can be beneficial for tracers with discontinuous profiles.

The modifications described here have been successfully tested in idealised case studies, weather forecast and atmospheric composition forecasts. Weather forecast test cases confirm that the algorithm remains positive definite and shape preserving with broadly neutral impact on forecast skill. The impact of the interpolation quasi-monotone limiter on water vapour transport, used by the IFS semi-Lagrangian scheme to ensure shape preservation, was analysed and its apparent moistening effect was explained. It was attributed to not allowing the cubic interpolation formula of the semi-Lagrangian advection scheme to generate new local minimum (undershoots) and local maximum (overshoots) values. Experiments show that the total mass which is effectively added in the atmosphere by clipping the undershoots exceeds the mass removed by clipping the overshoots. It was also shown that the 3D version of the available limiter is slightly more advantageous in terms of mass conservation.

Furthermore, high resolution CO_2 and CH_4 composition forecast tests showed that the octahedral grid reduces the mass conservation and transport error for these tracers and that an additional noticeable improvement is realised when the mass fixer is applied. However, in regions of the globe with strong surface fluxes, despite that the mass fixer correction is very small it may be comparable with the magnitude of anthropogenic emissions. This dictates the need for continuous monitoring of the performance of mass fixers and ideally the further improvement of the mass conservation properties of the underlying transport scheme to minimize uncertainties related with emissions.

Acknowledgements. The help of Dr. Sylvie Malardel in setting up the idealised bubble tests is gratefully acknowledged.

References

Agusti-Panareda, A., M. Diamantakis, V. Bayona, F. Klappenbach, and A. Butz (2017). Improving the inter-hemispheric gradient of total column atmospheric co2 and ch4 in simulations with the ECMWF semi-lagrangian atmospheric global model. *GMD 10*, 1–18.

Bermejo, R. and J. Conde (2002). A conservative quasi-monotone semi-Lagrangian scheme. *Mon. Weather Rev. 130*, 423–430.

Bermejo, R. and A. Staniforth (1992). The conversion of semi-Lagrangian advection schemes to quasi-monotone schemes. *Mon. Weather Rev. 120*, 2622–2631.

Diamantakis, M. and J. Flemming (2014). Global mass fixer algorithms for conservative tracer transport in the ECMWF model. *GMD 7*, 965–979.

Grandpre, J., M. Tanguay, A. Qaddouri, M. Zerroukat, and C. McLinden (2016). Semi-Lagrangian Advection of stratospheric Ozone on Yin-Yang grid system. *MWR 144*, 1035–1050.

Klappenbach, F., M. Bertleff, J. Kostinek, F. Hase, T. Blumenstock, A. Agusti-Panareda, M. Razinger, and A. Butz (2015). Accurate mobile remote sensing of xco_2 and xch_4 latitudinal transects from aboard a research vessel. *Atmospheric Measurement Techniques 8*, 5023–5038.

Malardel, S. and D. Ricard (2015). An alternative cell-averaged departure point reconstruction for pointwise semi-lagrangian transport schemes. *QJR 141*, 2114–2126.

Malardel, S., N. Wedi, W. Deconinck, M. Diamantakis, C. Kuehnlein, G. Mozdzynski, M. Hamrud, and P. Smolarkiewicz (2014). A new grid for the IFS. *ECMWF Newsletter No. 146 Winter 2015/16*, 23–28.

Ritchie, H., C. Temperton, A. Simmons, M. Hortal, T. Davies, D. Dent, and M. Hamrud (1995). Implementation of the semi-Lagrangian method in a high-resolution version of the ECMWF forecast model. *Mon. Weather Rev. 121*, 489–514.

Wunch, D., G. Toon, J.-F. L. Blavier, R. A. Washenfelder, J. Notholt, B. Connor, D. T. Griffith, V. Sherlock, and P. O. Wennberg (2011). The total carbon column observing network. *Phil. Trans. R. Soc. A 369*, 2087–2112.

Zerroukat, M. (2010). A simple mass conserving semi-Lagrangian scheme for transport problems. *J. Comput. Phys. 229*, 9011–9019.

A Appendix: Available IFS options for mass fixers

The following table describes the options available in IFS for controlling the different available mass fixer algorithms.

NAMGFL parameters	Type	Default value	Description
LTRCMFP	Logical	False	*Activate Proportional (PROP) MF*
LTRCMFMG	Logical	False	*Activate McGregor's (MG) MF*
LTRCMFBC	Logical	False	*Activate Bermejo-Conde (BC) MF*
LTRCMFPR	Logical	False	*Activate Priestley's (PR) MF*
Yxx_NL%LMASSFIX	Logical	False	*Activate MF on tracer xx*
NOPTMFBC	Integer (1,2,3,4)	1	Applies when LTRCMFBC=true *BC fixer type* 1: *standard qm BC MF* 2: *non-qm MF* 3: *multiplicative BC MF* 4: *multiplicative non-qm MF*
Yxx_NL%BETAMFBC	Real	1.0	Applies when LTRCMFBC=true *Specifies BC MF beta parameter to be applied on xx tracer.* Setting Yxx_NL%BETAMFBC<0 BC switches off BC MF for xx and uses proportional MF instead.
NOPTMFPR	Integer	1	Applies when Prietley's MF LTRCMFPR=true *PR MF type* 1: *apply qm-limiter before fixer acts* 2: *limiter is combined with PR MF i.e. quasi-monotone globally conserving field is computed at the same time (standard version of scheme but more expensive)*
LTRCMFIX_PS	Logical	False	Applies when any MF=true *Enforce global mass conservation on total air mass during SL advection. Mostly needed for CO2, CH4*
NMFDIAGLEV	Integer	0	*MF output level - diagnostic information printed in output file* 0: *no output* 1: *global mass diagnostics (useful for checking if mass fixer has been working as expected)* 2: detailed *global mass diagnostics + MF increment diagnostics*
NOPTVFE	Integer	0	Applies when any MF=true or NMFDIAGLEV>0 0: *Use simple finite difference pressure discretization when computing vertical mass integral for tracer (total column content) consistent with physics* 1: *Use finite element discretization consistent with dynamics*

Table 1. Tracer mass fixer options.

NAMDYN parameters	Type	Default	Description
LMASCOR	Logical	False	True: *Activate mass fixer for pressure* False: *No mass fixer applied on pressure (neither gridpoint or spectral)*
LMASDRY	Logical	False	Applies when LMASCOR=True True: *Activate dry MF for pressure* False: *Activate total mass (dry+wet) MF for pressure*
LGPMASCOR	Logical	False	This is the gridpoint mass fixer for pressure which applies when LMASCOR=True (replaces spectral MF) AND/OR when a tracer mass fixer used with LTRCMFIX_PS=true (enforces global mass conservation during SL advection). True: *Activate gridpoint MF for pressure* False: *Standard spectral MF is used if LMASCOR=true (otherwise no MF).* **NOTE:** When LGPMASCOR=true and a tracer mass fixers is used with LTRCMFIX_PS=true then global mass conservation is enforced not only on the tracer but on surface pressure advection and therefore on global mass of air as well. However, a further mass conservation error may be introduced at the end of the timestep due to semi-implicit correction which can be fixed by setting LMASCOR=true.
NGPMASCOR	Integer	0	Applies when LMASCOR=True and LGPMASCOR=True 0: *PROP MF for p* 1: *Zerroukat's MF for pressure computing correction weight depending on horizontal Laplacian of surface pressure. This is a more expensive option (uses extra spectral transform for p-surf)*
NAMCT0 parameters			
NFRMASSCON	Integer	32767	Frequency (in time steps) pressure MF is activated. Note that with default setting will remain inactive

Table 2. Pressure mass fixer options.